

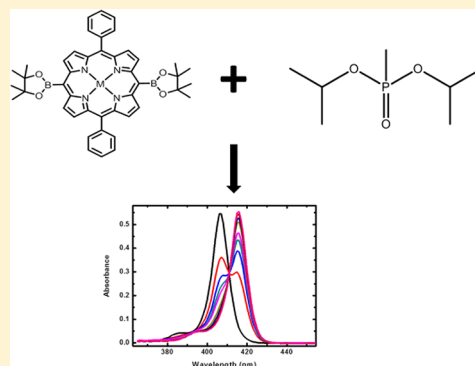
Spectroscopic Investigation of the Noncovalent Association of the Nerve Agent Simulant Diisopropyl Methylphosphonate (DIMP) with Zinc(II) Porphyrins

William A. Maza,[†] Carissa M. Vetromile,[‡] Chungsik Kim,[§] Xue Xu, X. Peter Zhang, and Randy W. Larsen*

Department of Chemistry, University of South Florida, 4202 East Fowler Avenue, Tampa, Florida 33620, United States

Supporting Information

ABSTRACT: Organophosphonates pose a significant threat as chemical warfare agents, as well as environmental toxins in the form of pesticides. Thus, methodologies to sense and decontaminate these agents are of significant interest. Porphyrins and metalloporphyrins offer an excellent platform to develop chemical threat sensors and photochemical degradation systems. These highly conjugated planar molecules exhibit relatively long-lived singlet and triplet states with high quantum yields and also form self-associated complexes with a wide variety of molecules. A significant aspect of porphyrins is the ability to functionalize the peripheral ring system either directly to the pyrrole rings or to the bridging methine carbons. In this report, steady-state absorption and fluorescence are utilized to probe binding affinities of a series of symmetric and asymmetric zinc(II) metalloporphyrins for the nerve agent simulant diisopropyl methylphosphonate (DIMP) in hexane. The red shifts in the absorption and emission spectra observed for all of the metalloporphyrins probed are discussed in the frame of Gouterman's four orbital model and a common binding motif involving coordination between the metalloporphyrin and DIMP via interaction between the zinc metal center of the porphyrin and phosphoryl oxygen of DIMP (Zn–O=P) is proposed.



INTRODUCTION

Weapons of mass destruction (WMD) continue to pose a significant threat despite being banned completely or tightly regulated/monitored. These weapon systems have remained a critical threat due to the presence of large stockpiles of chemical/biological weapons in countries that do not abide by international treaties and the availability of materials that can be utilized to construct primitive but effective biological/chemical weapons. Since these weapon systems remain a dangerous threat, methods to detect the use of these weapons as well as methods for decontamination subsequent to the weapons use are of critical importance.

Nerve agents (which affect the central nervous system by inhibiting the acetylcholine esterase) are typically organophosphonates based and include Tabun (ethyl *N,N*-dimethylphosphoramidocyanidate), Sarin (*O*-isopropyl methylphosphonofluoridate), Soman (*O*-pinacolyl methylphosphonofluoridate), and VX (methylphosphonothioic acid). Nerve agents irreversibly inhibit the acetylcholine esterase (AChE) thus preventing the hydrolysis of acetylcholine. Upon nerve activation acetylcholine is released from the presynaptic membrane associated with the cholinergic synapse and diffuses across the synaptic cleft binding to nicotinic acetylcholine receptors within the postsynaptic membrane. This results in an action potential that initiates rapid Ca^{2+} influx triggering muscle contraction. The AChE modulates the acetylcholine concentration via hydrolytic degradation to ensure that the

postsynaptic membrane is not overstimulated. Inhibition of AChE results in membrane overstimulation and involuntary muscle contractions ultimately leading to severe heart muscle arrhythmia.

Bacterial phosphotriesterases (PTE) have been shown to catabolize a variety of organophosphate compounds.^{1,2} The degradation mechanism has been proposed to occur via hydrolysis of the fluorenyl group of Sarin or Soman (or structurally equivalent substituent in other analogues).^{2,3} The active site comprises a binuclear Zn^{2+} metal center coordinated by four histidine residues and an aspartate residue and bridged by a carbamylated lysine residue.^{4,5} Recently, the crystal structure of PTE has been solved with the Sarin analogue/simulant diisopropyl methylphosphonate (DIMP) and indicates a mode of binding between DIMP and PTE via coordination of the phosphoryl oxygen to the more solvent exposed Zn^{2+} .³ A similar mode of binding to PTE has been observed with the simulant diethyl 4-methylbenzylphosphonate, though the tetrahedral coordination geometry of this complex differs from the distorted trigonal bipyramidal geometry of the DIMP-PTE complex.^{5,6} The ability of Zn^{2+} cation to coordinate to the phosphoryl oxygen provides a mechanism through which to develop colorimetric/fluorescence-based sensors as well as to

Received: June 17, 2013

Revised: September 16, 2013

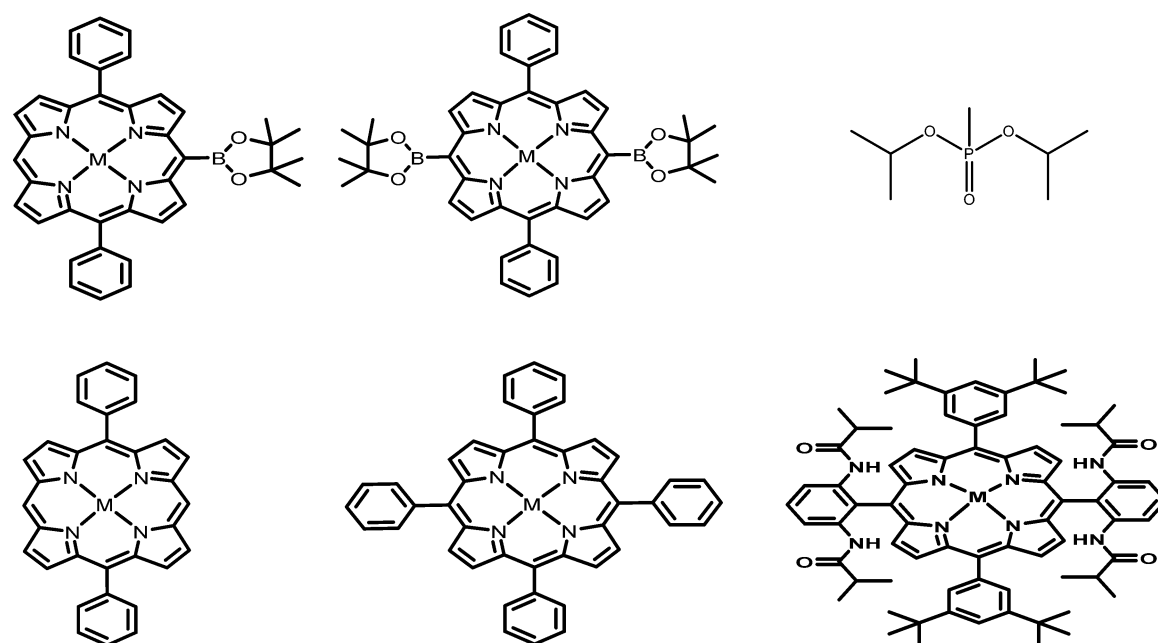


Figure 1. Structures of porphyrins examined for DIMP (top right) binding ($M = \text{Zn(II)}$). (Top left) 10-Monoborano-5,15-diphenylporphyrin, MBDPP, (top middle) 5,10-diborano-15,20-diphenylporphyrin, DBDPP, (bottom left) 5,10-diphenylporphyrin, DPP, (bottom middle) 5,10,15,20-tetraphenylporphyrin, TPP, (bottom right) 3,5-di-*t*Bu-IbuPhyrin, DtBIP.

facilitate decontamination of organophosphate toxins utilizing Zn^{2+} -based coordination complexes.

Colorimetric detection assays for the simulant, dimethyl methylphosphonate (DMMP), have recently been proposed based on a free-base tetraphenylporphyrin platform in polar solvents.^{7–9} The attraction of free-base and metalloporphyrins as sensor elements relies on their rich optical properties including large molar extinction coefficients in the UV (on the order of $1 \times 10^5 \text{ M}^{-1} \text{ s}^{-1}$) and visible regions (on the order of $1 \times 10^3 - 1 \times 10^4 \text{ M}^{-1} \text{ s}^{-1}$) and relatively good quantum yields of fluorescence for free-base and closed shell metalloporphyrins (up to ~ 0.20).^{10–13} These properties are a result of the conjugated electronic structure of the porphyrin macrocycle and, in the case of metalloporphyrins, the interactions between the macrocycle and metal center.^{14–19} Zinc(II) metalloporphyrins are of particular interest for sensing organophosphonates considering that the nature of the closed shell metal center allows for considerable fluorescence and a relatively long-lived triplet excited state as well as the role of Zn^{2+} ions in binding and hydrolysis of organophosphonates in phosphotriesterase proteins.^{1–6,20–24} However, other metalloporphyrins and corroles have also been shown to serve as sensor elements.^{25,26}

In the present study, the binding affinities of a variety of *meso*-substituted Zn^{2+} metalloporphyrins for DIMP (figure 1) are examined using steady-state absorption and fluorescence spectroscopy in hexane. The effect of the porphyrin structure on the binding affinity is considered and a preferred mode of binding is postulated.

MATERIALS AND METHODS

All solvents were purchased from Sigma-Aldrich and used without further purification. Diisopropyl methylphosphonate (DIMP) was purchased from Alfa Aesar and used as received. Porphyrin and DIMP stock solutions were freshly prepared in hexane prior to photometric titrations. Porphyrin sample

solutions were diluted in 1 cm^2 quartz cuvettes to $<10 \mu\text{M}$ in hexane and capped to minimize volume reduction due to solvent evaporation.

Steady-state UV–visible absorption spectra were collected using a Shimadzu UV-2401PC spectrophotometer. Steady-state emission spectra were collected using an ISS PC1 photon counting spectrophotometer using 0.5 mm slits on the excitation and emission monochromator. Samples were excited either at an isosbestic point between DIMP-bound and unbound porphyrin or, in the absence of a clear isosbestic point, at the porphyrin Soret maxima. Since no appreciable DIMP absorption was observed at the excitation or emission wavelengths, primary and secondary inner-filter effects were neglected and the emission spectra were normalized to the number of photons absorbed at the excitation wavelength.

Affinity constants were obtained by plotting the changes in absorption/emission as a function of DIMP concentration and fitting the data to Benesi–Hildebrand²⁷ expressions for absorption (eq 1) or emission (eq 2):

$$\Delta A_{\lambda} = \frac{K_a[\text{DIMP}]}{1 + K_a[\text{DIMP}]} [P]_0 \Delta \epsilon_{\lambda} \quad (1)$$

$$\Delta F_{\lambda} = \frac{K_a[\text{DIMP}]}{1 + K_a[\text{DIMP}]} (F_0 - F_{\infty}) \quad (2)$$

where K_a is the association constant for a one-to-one binding model, ΔA_{λ} and ΔF_{λ} are the changes in absorption and fluorescence intensity, respectively, at wavelength λ , $[P]_0$ is the total porphyrin concentration, $\Delta \epsilon_{\lambda}$ is the change in molar extinction at wavelength λ , and F_0 and F_{∞} are the fluorescence intensities in the absence of DIMP and at a saturating concentration of DIMP, respectively.

Synthesis of Zinc(II)[5,10,15,20-tetraphenylporphyrin] (ZnTPP). A solution of 5,10,15,20-tetraphenylporphyrin,²⁸ TPP (0.1 mmol), and $\text{Zn}(\text{OAc})_2 \cdot 4\text{H}_2\text{O}$ (0.3 mmol) in 2:1 chloroform/methanol (15 mL) was heated to reflux for 2 h.

The reaction mixture was cooled to room temperature, and the solvent was removed under reduced pressure. The desired Zn(II)porphyrin was purified by flash chromatography using chloroform as the eluent.

Synthesis of Zinc(II)[5,15-diphenylporphyrin] (ZnDPP). A solution of 5,10-diphenylporphyrin,²⁹ DPP (0.1 mmol) and Zn(OAc)₂·4H₂O (0.3 mmol) in HPLC grade chloroform (15 mL) was heated to reflux for 2 h. After cooling to room temperature, solvent was removed under reduced pressure. The desired Zn(II)porphyrin was obtained as a violet solid after purification by flash chromatography using chloroform as the eluent.

Synthesis of Zinc(II)[3,5-Di^tBu-lbuPhyrin] (ZnDtBIP). A solution of di^tBu-lbuPhyrin,³⁰ D^tBIP (0.1 mmol), and Zn(OAc)₂·4H₂O (0.3 mmol) in HPLC grade chloroform (15 mL) in the presence of triethylamine (TEA) was heated to reflux for 2 h. After cooling to room temperature, solvent was removed under reduced pressure. The desired Zn(II)porphyrin was purified by flash chromatography using chloroform as the eluent.

Synthesis of Zinc(II)[5-(4',4',5',5'-tetramethyl-[1',3',2']dioxaborolan-2'-yl)-10,20-diphenylporphyrin] (ZnMBDPP). A solution of 10-monoborano-5,15-diphenylporphyrin,³¹ MBDPP, (0.1 mmol) and Zn(OAc)₂·4H₂O (0.3 mmol) in the presence of triethylamine (TEA) in 10 mL dichloroethane was heated to reflux under N₂ for 2 h. The mixture was then cooled to room temperature. After quenching with NH₄Cl (aq) and washed with brine (2 times), the organic layer was dried with sodium sulfate (Na₂SO₄) before the solvent was evaporated. The desired Zn(II)porphyrin was isolated as a violet solid after purification by flash chromatography using chloroform as the eluent.

Synthesis of Zinc(II)[5,15-di-(4',4',5',5'-tetramethyl-[1',3',2']dioxaborolan-2'-yl)-10,20-diphenylporphyrin] (ZnDBDPP). A solution of 5,10-diborano-15,20-diphenylporphyrin,³¹ DBDPP (0.1 mmol), and Zn(OAc)₂·4H₂O (0.3 mmol) in 10 mL dichloroethane was heated to reflux under N₂ for 2 h. The mixture was then cooled to room temperature. After quenching with NH₄Cl (aq) and washed with brine (2 times), the mixture was dried with sodium sulfate (Na₂SO₄) before the solvent was evaporated. The desired Zn(II)porphyrin was isolated as a violet solid after purification by flash chromatography using chloroform as the eluent.

RESULTS

In general, bathochromic shifts in the absorption and emission spectra were observed for all of the Zn(II) porphyrins (i.e., ZnTPP, ZnDPP, ZnDBDPP, and ZnMBDPP) in the presence of DIMP although the shift in the emission spectra of ZnDBDPP was less pronounced than the others (see Figures 2–5). Specifically, the Soret band of ZnTPP shifts from 414 to 423 nm in the presence of ~1 mM DIMP and the Q-bands observed at 544 and 582 nm undergo bathochromic shifts to 558 and 596 nm, respectively (Figure 2). The emission bands observed at 591 and 639 nm shift to 603 and 656 nm, whereas the ratio of the intensities between the high energy emission band and low energy emission band increases from 0.39 in the absence of DIMP to 1.44 in the presence of ~1 mM DIMP. The ground state absorption and excited state emission spectra in the presence of ~1 mM DIMP resemble that of ZnTPP in neat acetonitrile and approach the spectra previously reported for ZnTPP in trimethylphosphate.³²

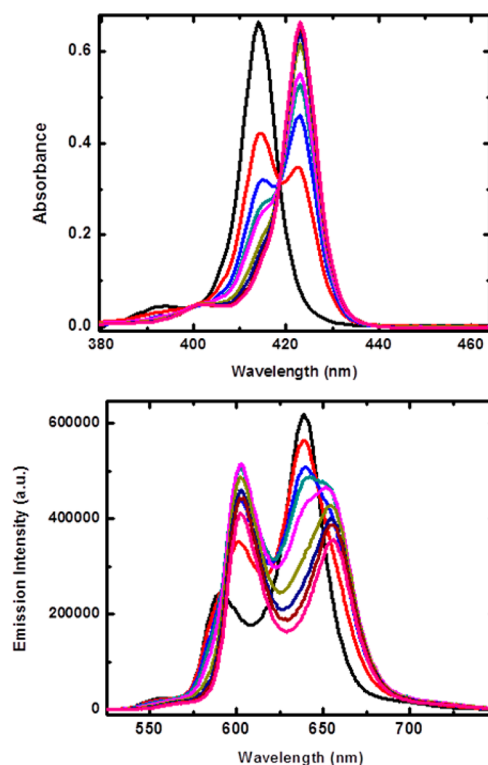


Figure 2. Top panel: Steady-state absorption spectra of ZnTPP in hexane as a function of DIMP concentration. Bottom panel: Corresponding steady-state emission spectra ($\lambda_{\text{exc}} = 418$ nm).

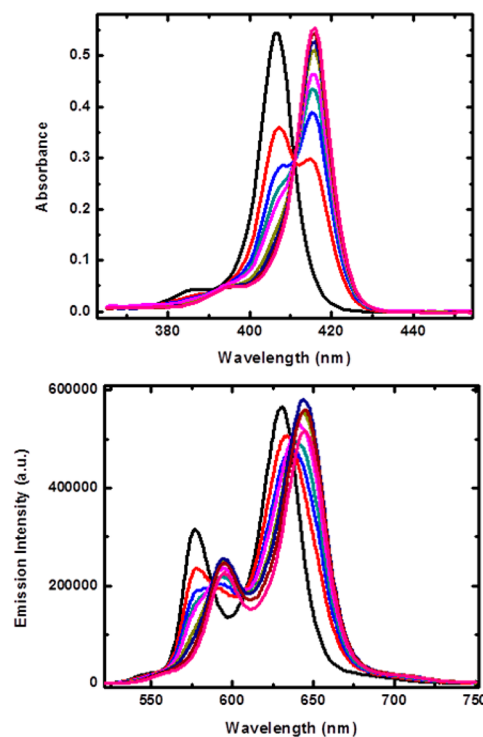


Figure 3. Top panel: Steady-state absorption spectra of ZnMBDPP in hexane as a function of DIMP concentration. Bottom panel: Corresponding steady-state emission spectra ($\lambda_{\text{exc}} = 411$ nm).

For ZnDPP, a bathochromic shift was also observed in the Soret shifting from 403 to 412 nm in the presence of ~1 mM DIMP with the Q-bands shifting to 545 and 582 nm from 532

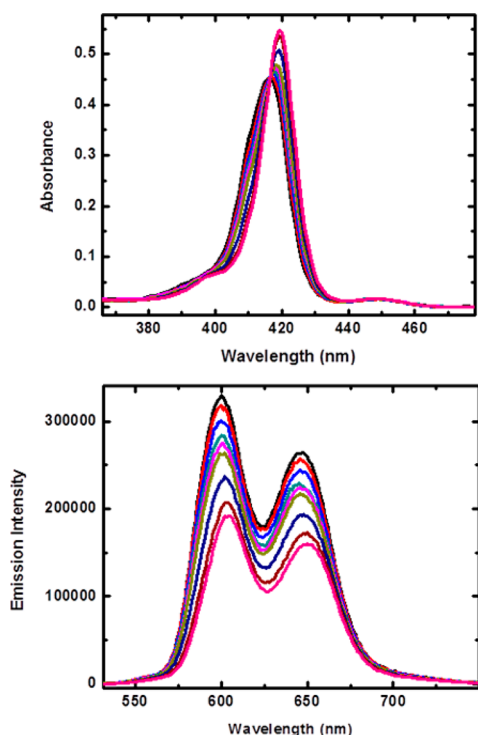


Figure 4. Top panel: Steady-state absorption spectra of ZnDBDPP in hexane as a function of DIMP concentration. Bottom panel: Corresponding steady-state emission spectra ($\lambda_{\text{exc}} = 419 \text{ nm}$).

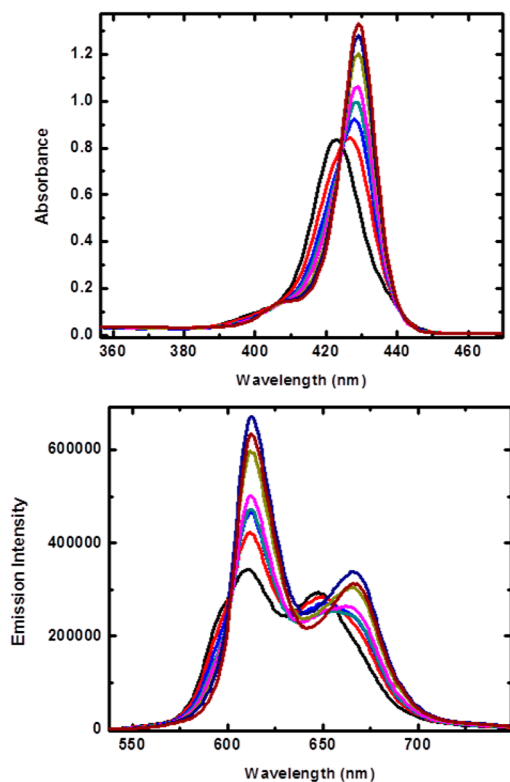


Figure 5. Top panel: Steady-state absorption spectra of ZnDtBIP in hexane as a function of DIMP concentration. Bottom panel: Corresponding steady-state emission spectra ($\lambda_{\text{exc}} = 424 \text{ nm}$).

and 567 nm. The emission bands display a shift from 571 and 623 nm to 587 and 638 nm upon addition of 1 mM DIMP. The ratio of the high energy/low energy emission band intensities

increases slightly from 0.35 to 0.47 in the presence of 1 mM DIMP.

Spectral changes similar to those of ZnDPP were observed for ZnMBDPP (Figure 3). The Soret band displayed a red shift to 416 nm from 407 nm and the emission bands shift from 577 and 631 nm to 594 and 644 nm in the presence of the same concentration of DIMP. However, despite the shift in emission the high energy/low energy emission band intensity ratio decreases slightly from 0.56 in the absence of DIMP to 0.44 in the presence of 1 mM DIMP. The corresponding ZnDBDPP (Figure 5) displays a red shift to 419 nm from 416 nm upon the addition of DIMP. However, the Q-band centered at 543 nm exhibited a slight hypsochromic shift to 539 nm while the 585 nm band shifted to 592 nm. The emission intensity significantly decreased with increasing concentration of DIMP and the emission bands were observed to red shift slightly from 600 and 647 nm to 604 and 650 nm.

The binding constants obtained from both absorption and emission data are summarized in Table 1. It was found from the

Table 1. DIMP Binding Affinities (in Terms of Association, K_a) for Zinc(II) Porphyrins in Hexane

porphyrin	absorbance	emission
	$K_a (10^4 \text{ M}^{-1})$	$K_a (10^4 \text{ M}^{-1})$
ZnDtBIP	1.50 ± 0.03	0.58 ± 0.05
ZnDBDPP	0.41 ± 0.02	0.28 ± 0.02
ZnMBDPP	2.09 ± 0.04	1.4 ± 0.20
ZnDPP	2.51 ± 0.03	1.94 ± 0.09
ZnTPP	2.17 ± 0.07	0.37 ± 0.04

changes in the absorption spectra that all zinc(II) metalloporphyrins exhibited similar binding affinities with K_a values between 1.5×10^4 and $2.5 \times 10^4 \text{ M}^{-1}$. The notable exception is ZnDBDPP, which has a K_a of $4.1 \times 10^3 \text{ M}^{-1}$. The affinity constants obtained from emission measurements, however, were markedly different from those obtained by absorption. In general the binding affinities were observed to decrease upon generation of the porphyrin singlet excited state. The origin of these differences is discussed below.

DISCUSSION

Steady-State Absorption. The optical spectrum of metalloporphyrins provides important information regarding the ligation, oxidation, and spin state of the central metal as well as the polarity of the porphyrin's solvent environment. Under D_{4h} symmetry the lowest occupied MOs of the porphyrin are of a_{1u} and a_{2u} symmetry with a degenerate set of orbitals with e_g symmetry comprising the lowest unoccupied molecular orbital (LUMO). The porphyrin optical spectrum for these systems is best described using a four orbital model, originally proposed by Gouterman,^{14–24} that involves extensive configuration interaction between the nearly degenerate a_{2u} and a_{1u} highest occupied orbitals (HOMOs) and the degenerate set of e_g^* LUMOs.^{14–24,33} The ground state of the D_{4h} porphyrin π -system has an electron configuration of $\dots(a_{2u})^2(a_{1u})^2$ producing an $^1A_{1g}$ state. The excited electron configurations $\dots(a_{2u})^2(a_{1u})^1(e_g)^1$, $\dots(a_{2u})^2(a_{1u})^1(e_g)^1$, $\dots(a_{2u})^1(a_{1u})^2(e_g)^1$, and $\dots(a_{2u})^1(a_{1u})^2(e_g)^1$ interact via the two electron repulsion term $H' = e'^2/r_{ij}$, to give an energy level diagram where A_{1g}' is the average energy splitting of the a_{2u} and a_{1u} orbitals and A_{1g}'' is the matrix element that couples the excited electron

configurations (e.g., $\langle (a_{1u}e_g)|H|(a_{2u}e_g) \rangle$).^{20–24} Transitions between these states give rise to the B- and Q-band transitions and accurately reflect the difference in molar extinction coefficient.^{14–19,33} Introduction of a transition metal atom to the porphyrin core results in shifts in the relative energies of the a_{2u}/a_{1u} orbital energies, thus affecting the A_{1g}' matrix element and the B- and Q-band positions.^{20–24} In addition, the 3d orbitals of the metal can also interact directly with porphyrin molecular orbitals of the same symmetry. Since the metal orbitals transform as b_{1g} ($3d_{x^2-y^2}$), a_{1g} ($3d_{z^2}$), b_{2g} ($3d_{xy}$), e_g ($3d_{xz}$, $3d_{yz}$) in D_{4h} , only the e_g ($3d_{xz}$, $3d_{yz}$) orbitals can mix with the porphyrin e_g^* (π -orbitals). Occupancy of the metal $3d_{xz}$ and $3d_{yz}$ orbitals can then influence the electronic properties of the metalloporphyrin.

Upon the addition of DIMP, the Soret and Q-band absorption maxima of the Zn^{2+} complexes of porphyrins all red-shifted. These shifts are similar to those previously observed for the coordination of N, S, O, and P-containing ligands to ZnTPP.^{34–36} Interestingly, ZnTPP, ZnDPP, and ZnMBDPP each displayed a 9 nm red-shift in the Soret band. The Soret band red-shift observed for ZnDBDPP and ZnDtBIP is less pronounced, however, shifting only 3 and 6 nm, respectively. Nappa and Valentine³⁵ have proposed that the observed red-shifts upon coordination of varying Lewis base ligands (of S-, N-, O-, or P-containing donors) for ZnTPP are less dependent on the strength of the interaction between the zinc(II) and the ligand and more on the basicity of the ligand. According to Gouterman, decreased electronegativity on the central metal atom increases electron density of the p_π orbitals of the porphyrin macrocycle and in turn increases the energy of the a_{2u} orbital, thereby decreasing the $a_{2u} \rightarrow e_g$ transition energy.¹⁴ Nappa and Valentine further speculated that upon coordination of a ligand of sufficient electron-donating propensity, density in the p_π orbital of the porphyrin is increased by conjugative effects via the zinc(II) metal center.³⁵

Steady-State Emission. The observed emission spectra for each zinc(II) porphyrin examined in the absence of DIMP display two transitions between 550 and 750 nm, which correspond to the Q(0,0) transition (typically between 550 and 620 nm) and the Q(0,1) transition (between 620 and 700 nm). The emission Q-band maxima for the metalloporphyrins probed are listed in Table 2. In general, bathochromic shifts were noted in the maxima corresponding to the two Q-band

Table 2. Absorbance and Emission Maxima for the Unbound and DIMP Bound Metalloporphyrins

	absorption			emission	
	Soret (B)	Q(0,0)	Q(0,1)	Q(0,0)	Q(0,1)
ZnTPP	414 nm	582 nm	544 nm	591 nm	639 nm
ZnTPP + DIMP	423 nm	596 nm	558 nm	603 nm	656 nm
ZnDPP	403 nm	567 nm	532 nm	571 nm	623 nm
ZnDPP + DIMP	412 nm	582 nm	545 nm	587 nm	638 nm
ZnMBDPP	407 nm	571 nm	537 nm	577 nm	631 nm
ZnMBDPP + DIMP	416 nm	584 nm	549 nm	594 nm	644 nm
ZnDBDPP	416 nm	584 nm	542 nm	600 nm	647 nm
ZnDBDPP + DIMP	419 nm	591 nm	539 nm	604 nm	650 nm
ZnDtBIP	423 nm	604 nm	549 nm	611 nm	648 nm
ZnDtBIP + DIMP	429 nm	606 nm	560 nm	613 nm	666 nm

transitions upon the addition of DIMP. No significant quenching of the fluorescence was observed with the exception of ZnDBDPP. In fact, the red shift observed in the emission spectra of ZnDtBIP was accompanied by an increase in emission intensity with added DIMP. The changes in intensity as a function of DIMP concentrations were fit to eq 2 to obtain the corresponding association constants of the metalloporphyrins for DIMP. These values are also summarized in Table 1.

Interestingly, the red shift corresponding to formation of the metalloporphyrin:DIMP complex is accompanied by a change in the Q(0,0)/Q(0,1) intensity ratio, though the direction and degree of the change varied between metalloporphyrins. For example, in the case of ZnTPP the Q(0,0) band increased in intensity while a significant decrease in intensity was observed for the Q(0,1) band. In the case of ZnDPP, both the Q(0,0) and the Q(0,1) bands were observed to increase in intensity, though disproportionately. Formation of the ZnDBDPP:DIMP complex resulted in a decrease in intensities of both transitions, though slightly disproportionately. ZnMBDPP displayed a marked decrease in the Q(0,0) intensity with an almost negligible increase in the Q(0,1) intensity upon association with DIMP. DIMP complexation with ZnDtBIP resulted in a narrowing of the Q(0,0) band and an intensity increase of both Q(0,0) and Q(0,1) transitions.

The intensity of transitions between vibronic manifolds of two electronic states such as Q(0,0) and Q(0,1) of the $S_1 \rightarrow S_0$ electronic transitions depends on the degree of overlap between the nuclear wave functions corresponding to the two vibrational states according to

$$F_{i \rightarrow j} = C_i R_{e \rightarrow g}^2 \langle j|i \rangle^2 \quad (3)$$

where $R_{e \rightarrow g}$ is the electronic transition moment between the porphyrin S_1 excited state and S_0 ground state, C is a constant dependent on the population density of the excited state vibrational manifold, i , and $\langle j|i \rangle$ is the nuclear overlap integral between the excited state vibrational manifold, i , and ground state vibrational manifold, j . The data suggests that binding of DIMP to each metalloporphyrin affects the Q(0,0) and Q(0,1) transition of the corresponding porphyrin differently by either increasing or decreasing the ij overlap integral. The fact that the relative spacing between the Q(0,0) and Q(0,1) transitions as well as the change in Stokes shifts were essentially the same for ZnTPP, ZnDPP, and ZnMBDPP in the absence and presence of DIMP (Table 2) is indicative of a common binding motif, which presumably involves the zinc(II) metal center. However, the relative orientations between the DIMP and porphyrin macrocycle may differ between the porphyrin species leading to the changes observed in the emission intensities of the transitions. Differences in the orientation and/or vibrational overlap may arise from electronic (inductive or Coulombic) effects related to the properties of the porphyrin substituents at the *meso*-positions or steric factors. Distortion of the planarity of the porphyrin macrocycle upon ligand binding may also perturb the energies of the a_{2u} , a_{1u} and/or e_g orbitals. Crystal structures of 5-coordinate complexes of ZnTPP and some O-donating ligands, such as dimethylformamide and dimethylacetamide, result in distortions of the porphyrin macrocycle planarity while coordination of dimethylsulfoxide to the ZnTPP macrocycle results in a relatively planar conformation.^{36–39}

Plots of the ratio of the intensity of the Q(0,0) transition in the absence of DIMP, F_o , to the intensity of the same transition in the presence of DIMP, F , as a function of DIMP

concentration were nonlinear displaying downward curvatures in all cases. Downward curvature is indicative of the presence of multiple emissive components in solution. It is likely that these emissive species correspond to DIMP-bound and unbound porphyrins in solution. If diffusional (collisional) quenching of the zinc(II) porphyrin fluorescence is negligible, and the resulting complex is emissive, a plot of F_0/F can be expressed as

$$\frac{F_0}{F} = \frac{1 + K_a[\text{DIMP}]}{1 + \left(\frac{\tau_0}{\tau'}\right)K_a[\text{DIMP}]} \quad (4)$$

where τ_0 is the fluorescence lifetime of the unbound porphyrin, τ' is the fluorescence lifetime of the bound porphyrin, and K_a is the association constant. Fits of the data to eq 4 are presented in Table 3, and the K_a s obtained agree very well with those

Table 3. Summary of Fluorescence Titration Data Fits to eq 4

porphyrin	K_a (10^4 M^{-1})	τ_0 (ns)	τ' (ns)
ZnDtBIP	0.55	1.14	2.42
ZnDBDPP	0.29	0.78	0.32
ZnMBDPP	1.44	1.30	0.82
ZnDPP	1.91	1.05	0.63
ZnTPP	0.45	1.82	0.34

given in Table 1. The fluorescence lifetime value (~ 1.9 ns) extracted from the fit for unbound ZnTPP was found to agree with that measured experimentally in benzene and methylcyclohexane (~ 1.5 – 1.8 ns).^{22,40,41}

A marked difference in the binding affinities obtained by a Benesi–Hildebrand treatment of the steady-state absorption and steady-state emission data for the interaction between the Zn(II) metalloporphyrins probed and DIMP was noted above. The results obtained from fits of the emission data to eq 4 confirm the validity of the values obtained from eq 2. However, the origin of the differences in affinities is not immediately apparent. Previous studies involving ligand binding to ZnTPP have attributed Lewis acid properties to the metalloporphyrin and have noted that the binding affinity of ZnTPP with Lewis base-type ligands correlate well with the strength of the base (where deviations due to sterics were not considered).^{31,36,42,43} The decreased affinity constants obtained from the emission data are, therefore, likely to be due to a decrease in the Lewis acid character of the metal center in ZnTPP upon generation of the excited state.^{44,45} In fact, Lampa-Pastirk et al.⁴⁵ have noted stepwise photodissociation of the axial ligands in Zn(II)-substituted cytochrome c upon excitation at the zinc porphyrin Soret band.

Proposed Binding Motif. A wide variety of oxygen-containing ligands, including phosphine based ligands, have previously been shown to bind to ZnTPP in solvents of varying polarity with reasonable affinity (i.e., down to $K_d \approx 1.4$ mM for dimethylsulfoxide).^{34,45–50} The primary mode of binding between Zn based porphyrins and phosphonates is through the phosphoryl oxygen and the porphyrin zinc metal center, $\text{P}=\text{O}\cdots\text{Zn}$.^{26,45–50} A similar mode of interaction has been observed in crystal structures of ZnTPP and O-donating ligands such as dimethylsulfoxide, dimethylformamide, and dimethylacetamide^{36–38} as well as open shell metalloporphyrins and corroles.²⁵ Two geometries are possible for the $\text{P}=\text{O}\cdots\text{Zn}$ binding mode with $((\text{CH}_3)_2\text{CHO})_2(\text{CH}_3)\text{P}=\text{O}$ as a ligand (Figure 6). The first is a gauche conformation in which the

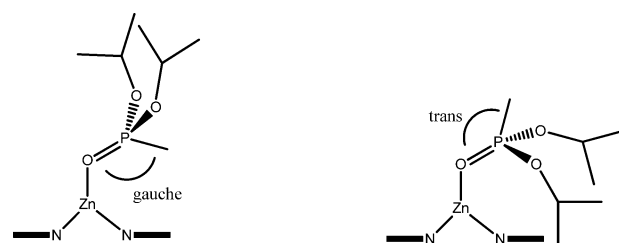


Figure 6. Two different binding modes between Zn(II) porphyrins and DIMP.

DIMP methyl group lies adjacent to the plane of the porphyrin macrocycle and the second is a trans conformation in which the DIMP methyl group is directed away from the porphyrin macrocycle.

Preliminary electrostatic surface potential calculations performed with HyperChem using the PM3 method (see Supporting Information) indicate (1) a positive electrostatic surface is prominent over the phosphoryl oxygen groups of DIMP, (2) a large positive electrostatic surface over the face of the parent macrocycle of zinc porphyrin, and (3) that the surface potential is diminished in the ZnMBDPP, ZnDBDPP, and ZnDtBIP macrocycles. It is proposed that the relative orientation of the DIMP methyl group is gauche to the $\text{P}=\text{O}\cdots\text{Zn}$ interaction such that the DIMP alkoxy groups are directed away from the metalloporphyrin macrocycle thereby minimizing the Coulombic repulsion between the electrostatic surfaces of the alkoxy groups and the interior potential of the porphyrin macrocycle.

SUMMARY

Steady-state absorption and emission were used to probe the binding and affinity constants for the nerve agent simulant DIMP to a series of zinc(II) metalloporphyrins. In each case, red shifts were observed in both the absorption and emission spectra upon binding of DIMP. The magnitudes of the red shift are attributed to inductive donation of electronic density from the basic phosphoryl oxygen of DIMP into the porphyrin p_π macrocycle via the zinc(II) metal center. It is proposed that the binding of DIMP to the metalloporphyrins occurs via the DIMP phosphoryl oxygen and the porphyrin zinc(II) metal center where the DIMP alkoxy groups are directed away from the porphyrin macrocycle core. The resulting binding affinities in hexane resembles that of some relatively strong N-donating bases for ZnTPP in noncoordinating solvents and generally diminish for the bulkier substituted porphyrins. The decrease in affinity is attributed to a decrease in acidity of the porphyrin at the porphyrin macrocycle core; possibly an effect of the nature of the substituent.

ASSOCIATED CONTENT

Supporting Information

Derivation of eq 4 as well as ZnPorphyrin-DIMP binding curves and fits to eq 4. This material is available free of charge via the Internet at <http://pubs.acs.org>.

AUTHOR INFORMATION

Corresponding Author

*(R.W.L.) E-mail: rwlarsen@usf.edu. Phone: 813 974 7925.

Present Addresses

[†]Department of Chemistry, Virginia Polytechnic Institute and State University (Virginia Tech.), 306 Hahn Hall North, Blacksburg, Virginia 24061, United States.

[‡]Department of Cell and Molecular Biology, University of Hawaii Manoa, 651 Ilalo Street, BSB 222, Honolulu, Hawaii 96813, United States.

[§]Department of Chemistry, Kyushu University, Japan.

Notes

The authors declare no competing financial interest.

ACKNOWLEDGMENTS

This work was supported by the Department of Defense–Defense Threat Reduction Agency (DoD–DTRA) through HDTRA1-08-C-0035.

REFERENCES

- (1) Caldwell, S. R.; Raushel, F. M. Detoxification of Organophosphate Pesticides Using a Nylon Based Immobilized Phosphotriesterase from *Pseudomonas-Diminuta*. *Appl. Biochem. Biotechnol.* **1991**, *31*, 59–73.
- (2) Dumas, D. P.; Caldwell, S. R.; Wild, J. R.; Raushel, F. M. Purification and Properties of the Phosphotriesterase from *Pseudomonas-Diminuta*. *J. Biol. Chem.* **1989**, *264*, 19659–19665.
- (3) Benning, M. M.; Hong, S. B.; Raushel, F. M.; Holden, H. M. The Binding of Substrate Analogs to Phosphotriesterase. *J. Biol. Chem.* **2000**, *275*, 30556–30560.
- (4) Omburo, G. A.; Kuo, J. M.; Mullins, L. S.; Raushel, F. M. Characterization of the Zinc-Binding Site of Bacterial Phosphotriesterase. *J. Biol. Chem.* **1992**, *267*, 13278–13283.
- (5) Benning, M. M.; Kuo, J. M.; Raushel, F. M.; Holden, H. M. Three-Dimensional Structure of the Binuclear Metal Center of Phosphotriesterase. *Biochemistry* **1995**, *34*, 7973–7978.
- (6) Vanhooke, J. L.; Benning, M. M.; Raushel, F. M.; Holden, H. M. Three-Dimensional Structure of the Zinc-Containing Phosphotriesterase with the Bound Substrate Analog Diethyl 4-Methylbenzylphosphonate. *Biochemistry* **1996**, *35*, 6020–6025.
- (7) Cao, H. T.; Nam, J.; Harmon, H. J.; Branson, D. H. Spectrophotometric Detection of Organophosphate Diazinon by Porphyrin Solution and Porphyrin-Dyed Cotton Fabric. *Dyes Pigm.* **2007**, *74*, 176–180.
- (8) Huo, D. Q.; Yang, L. M.; Hou, C. J.; Fa, H. B.; Luo, X. G.; Lu, Y.; Zheng, X. L.; Yang, J.; Yang, L. Molecular Interactions of Monosulfonate Tetraphenylporphyrin (TPPS1) and Meso-Tetra(4-sulfonatophenyl)porphyrin (TPPS) with Dimethyl Methylphosphonate (DMMP). *Spectrochim. Acta, Part A* **2009**, *74*, 336–343.
- (9) Zhang, S. Y.; Yang, L. M.; Huo, D. Q.; Liu, X. J.; Li, J.; Fa, H. B.; Zhang, L.; Hou, C. J. Molecular Interactions of Dimethyl Methylphosphonate (DMMP) with Metalloporphyrins: Determination of the Binding Mechanism by Spectroscopic Methods. *Spectrochim. Acta, Part A* **2012**, *88*, 137–143.
- (10) Beer, P. D.; Cormode, D. P.; Davis, J. J. Zinc Metalloporphyrin-Functionalised Nanoparticle Anion Sensors. *Chem. Commun.* **2004**, 414–415.
- (11) Di Natale, C.; Macagnano, A.; Repole, G.; Saggio, G.; D'Amico, A.; Paolesse, R.; Boschi, T. The Exploitation of Metalloporphyrins as Chemically Interactive Material in Chemical Sensors. *Mater. Sci. Eng. C* **1998**, *5*, 209–215.
- (12) Gorski, L.; Malinowska, E.; Parzuchowski, P.; Zhang, W.; Meyerhoff, M. E. Recognition of Anions Using Metalloporphyrin-Based Ion-Selective Membranes: State-of-the-Art. *Electroanalysis* **2003**, *15*, 1229–1235.
- (13) Malinowska, E.; Niedziolka, J.; Meyerhoff, M. E. Potentiometric and Spectroscopic Characterization of Anion Selective Electrodes Based on Metal(III) Porphyrin Ionophores in Polyurethane Membranes. *Anal. Chim. Acta* **2001**, *432*, 67–78.
- (14) Gouterman, M. Study of the Effects of Substitution on the Absorption Spectra of Porphin. *J. Chem. Phys.* **1959**, *30*, 1139–1161.
- (15) Gouterman, M. Spectra of Porphyrins. *J. Mol. Spectrosc.* **1961**, *6*, 138–163.
- (16) Gouterman, M.; Snyder, L. C.; Wagniere, G. H. Spectra of Porphyrins. 2. 4 Orbital Model. *J. Mol. Spectrosc.* **1963**, *11*, 108–127.
- (17) Liao, M. S.; Scheiner, S. Electronic Structure and Bonding in Metal Porphyrins, (Metal = Fe, Co, Ni, Cu, Zn). *J. Chem. Phys.* **2002**, *117*, 205–219.
- (18) Shelnutz, J. A.; Ortiz, V. Substituent Effects on the Electronic-Structure of Metalloporphyrins: A Quantitative-Analysis in Terms of 4-Orbital-Model Parameters. *J. Phys. Chem.* **1985**, *89*, 4733–4739.
- (19) Weiss, C.; Kobayash, H.; Gouterman, M. Spectra of Porphyrins. 3. Self-Consistent Molecular Orbital Calculations of Porphyrins and Related Ring Systems. *J. Mol. Spectrosc.* **1965**, *16*, 415–450.
- (20) Whitten, D. Photochemistry of Porphyrins and Their Metal Complexes in Solution and Organized Media. *Res. Chem. Intermed.* **1978**, *2*, 107–138.
- (21) Harriman, A. Luminescence of Porphyrins and Metalloporphyrins. 1. Zinc(II), Nickel(II), and Manganese(II) Porphyrins. *J. Chem. Soc., Faraday Trans. 1* **1980**, *76*, 1978–1985.
- (22) Harriman, A. Luminescence of Porphyrins and Metalloporphyrins. 3. Heavy-Atom Effects. *J. Chem. Soc., Faraday Trans. 2* **1981**, *77*, 1281–1291.
- (23) Harriman, A.; Hosie, R. J. Luminescence of Porphyrins and Metalloporphyrins. 4. Fluorescence of Substituted Tetraphenylporphyrins. *J. Chem. Soc., Faraday Trans. 2* **1981**, *77*, 1695–1702.
- (24) Krasnovsky, A. A.; Venediktov, E. A. Quenching of Singlet Oxygen Luminescence by Porphyrins and Metalloporphyrins. *Biofizika* **1978**, *23*, 387–389.
- (25) Kim, K.; Kim, I.; Maiti, N.; Kwon, S. J.; Bucella, D.; Egorova, O. A.; Lee, Y. S.; Kwak, J.; Churchill, D. G. A Study of Nerve Agent Model Organophosphonates Binding with Manganese-A2B-Corrole and A2B2-Porphyrin Systems. *Polyhedron* **2009**, *28*, 2418–2430.
- (26) Kim, K.; Tsay, O. G.; Atwood, D. A.; Churchill, D. G. Destruction and Detection of Chemical Warfare Agents. *Chem. Rev.* **2011**, *111*, 5345–5403.
- (27) Benesi, H. A.; Hildebrand, J. H. A Spectrophotometric Investigation of the Interaction of Iodine with Aromatic Hydrocarbons. *J. Am. Chem. Soc.* **1949**, *71*, 2703–2707.
- (28) Adler, A. D.; Longo, F. R.; Kampas, F.; Kim, J. On the Preparation of Metalloporphyrins. *J. Inorg. Nucl. Chem.* **1970**, *32*, 2443–2445.
- (29) Frail, P. R.; Susumu, K.; Huynh, M.; Fong, J.; Kikkawa, J. M.; Therien, M. J. Modulation of Dark Conductivity over a 1×10^{-12} to 1×10^{-5} S/cm Range through Ancillary Group Modification in Amorphous Solids of Ethyne-Bridged (Porphinato)zinc(II) Oligomers. *Chem. Mater.* **2007**, *19*, 6062–6064.
- (30) Ruppel, J. V.; Jones, J. E.; Huff, C. A.; Kamble, R. M.; Chen, Y.; Zhang, X. P. A Highly Effective Cobalt Catalysts for Olefin Aziridination with Azides: Hydrogen Bonding guided Catalyst Design. *Org. Lett.* **2008**, *10*, 1995–1998.
- (31) Hyslop, A. G.; Kellett, M. A.; Iovine, P. M.; Therien, M. J. Suzuki Porphyrins: New Synthons for the Fabrication of Porphyrin-Containing Supramolecular Assemblies. *J. Am. Chem. Soc.* **1998**, *120*, 12676–12677.
- (32) Humphry-Baker, R.; Kalyanasundaram, K. Influence of Axial Ligation on the Fluorescence of Tetrakisphenylporphyrins. *J. Photochem.* **1985**, *31*, 105–112.
- (33) Owens, J. W.; Smith, R.; Robinson, R.; Robins, M. Photo-physical Properties of Porphyrins, Phthalocyanines, and Benzochlorins. *Inorg. Chim. Acta* **1998**, *279*, 226–231.
- (34) Kolling, O. W. Soret Red Shift for Zinc Tetraphenylporphyrin in the Presence of Uncharged Lewis-Bases. *Inorg. Chem.* **1979**, *18*, 1175–1176.
- (35) Nappa, M.; Valentine, J. S. Influence of Axial Ligands on Metalloporphyrin Visible Absorption Spectra: Complexes of Tetraphenylporphyrinatozinc. *J. Am. Chem. Soc.* **1978**, *100*, 5075–5080.

(36) Vogel, G. C.; Stahlbush, J. R. Thermodynamic Study of the Adduct Formation of Zinc Tetraphenylporphine with Several Neutral Donors in Cyclohexane. *Inorg. Chem.* **1977**, *16*, 950–953.

(37) Vinodu, M.; Goldberg, I. A Dimethyl Sulfoxide/Chloroform Clathrate of (Dimethyl Sulfoxide) (Tetraphenylporphyrinato)zinc(II). *Acta Crystallogr., Sect. E: Struct. Rep. Online* **2004**, *60*, m579–m581.

(38) Lipstman, S.; Muniappan, S.; Goldberg, I. (Dimethylacetamide)-(tetraphenylporphyrinato)zinc(II). *Acta Crystallogr., Sect. E: Struct. Rep. Online* **2006**, *62*, m2330–2332.

(39) Lipstman, S.; Goldberg, I. Unsolvated (Dimethylformamide)-(tetraphenylporphyrinato)zinc(II). *Acta Crystallogr., Sect. E: Struct. Rep. Online* **2006**, *62*, m158–m160.

(40) Yu, H. Z.; Baskin, J. S.; Zewail, A. H. Ultrafast dynamics of Porphyrins in the Condensed Phase. II. Zinc Tetraphenylporphyrin. *J. Phys. Chem. A* **2002**, *106*, 9845–9854.

(41) Seybold, P. G.; Gouterman, M. Porphyrins. 13. Fluorescence Spectra and Quantum Yields. *J. Mol. Spectrosc.* **1969**, *31*, 1–13.

(42) Vogel, G. C.; Searby, L. A. Lewis Acid-Base Interactions of Zinc Alpha, Beta, Gamma, Delta-Tetraphenylporphine with Several Neutral Donors. *Inorg. Chem.* **1973**, *12*, 936–939.

(43) Mizutani, T.; Kurahashi, T.; Murakami, T.; Matsumi, N.; Ogoshi, H. Molecular Recognition of Carbohydrates by Zinc Porphyrins: Lewis Acid Lewis Base Combinations as a Dominant Factor for their Selectivity. *J. Am. Chem. Soc.* **1997**, *119*, 8991–9001.

(44) Lampa-Pastirk, S.; Lafuente, R. C.; Beck, W. F. Excited-State Axial-Ligand Photodissociation and Nonpolar Protein-Matrix Reorganization in Zinc(II)-Substituted Cytochrome C. *J. Phys. Chem. B* **2004**, *108*, 12602–12607.

(45) Lin, C. L.; Fang, M. Y.; Cheng, S. H. Substituent and Axial Ligand Effects on the Electrochemistry of Zinc Porphyrins. *J. Electroanal. Chem.* **2002**, *531*, 155–162.

(46) Nardo, J. V.; Dawson, J. H. Spectroscopic Evidence for the Coordination of Oxygen Donor Ligands to Tetraphenylporphyrinato-zinc. *Inorg. Chim. Acta* **1986**, *123*, 9–13.

(47) Enakieva, Y. Y.; Bessmertnykh, A. G.; Gorbunova, Y. G.; Stern, C.; Rousselin, Y.; Tsivadze, A. Y.; Guillard, R. Synthesis of meso-Polyphosphorylporphyrins and Example of Self Assembling. *Org. Lett.* **2009**, *11*, 3842–3845.

(48) Chekmeneva, E.; Hunter, C. A.; Packer, M. J.; Turega, S. M. Evidence of Partially Bound States in Cooperative Molecular Recognition Interfaces. *J. Am. Chem. Soc.* **2008**, *130*, 17718–17725.

(49) Officer, D. L.; Lodato, F.; Jolley, K. W. Zinc-Porphyrin Phosphonate Coordination: Structural Control through a Zinc Phosphoryl–Oxygen Interaction. *Inorg. Chem.* **2007**, *46*, 4781–4783.

(50) Matano, Y.; Matsumoto, K.; Terasaka, Y.; Hotta, H.; Araki, Y.; Ito, O.; Shiro, M.; Sasamori, T.; Tokitoh, N.; Imahori, H. Synthesis, Structures and Properties of meso-Phosphorylporphyrins: Self-Organization through P-Oxo-Zinc Coordination. *Eur. J. Chem.* **2007**, *13*, 891–901.